Fast Imaging of Partially Conductive Linear Cracks Using Impedance Data

Kurt Bryan,‡ Janine Haugh,§ and David McCune‖

Abstract. We develop two closely-related fast and simple numerical algorithms to address the inverse problem of identifying a collection of disjoint linear cracks in a two-dimensional homogeneous electrical conductor from exterior boundary voltage/current measurements. We allow the possibility that the cracks are partially conductive. Our approach also allows us to determine the actual number of cracks present, as well as make use of one or multiple input fluxes. We illustrate our algorithms with a variety of computational examples.

Keywords: inverse problem, impedance imaging, cracks, transmission condition, reciprocity gap.
AMS subject classifications: 35R30

1. Introduction

Impedance imaging remains a topic of considerable activity in the inverse problems community. Of special interest are algorithms that make use of a priori information or assumptions concerning the nature of the target's internal structure. Such assumptions can usually be exploited to obtain much faster, simpler, and more stable algorithms than would otherwise be possible. In this paper we consider the problem of determining the number and location of a collection of linear cracks inside a homogeneous conductor, under the assumption that the cracks may allow partial conduction across their boundaries.

The impedance imaging problem for cracks was first considered in [15]. In that paper the authors prove a uniqueness result for the problem, specifically, that any perfectly insulating or conductive crack in a two-dimensional region with real-analytic background conductivity can be uniquely determined using the "measured" boundary potentials (Dirichlet data) corresponding to two input current fluxes (Neumann data) of a certain type. The authors also show that one input flux may not suffice. Independently, the authors of [2] and [17] show that two appropriate input-flux/boundary-potential pairs suffice to identify any finite collection of cracks.

‡ Department of Mathematics, Rose-Hulman Institute of Technology, Terre Haute, IN 47803. This work was partially supported by an NSF-REU grant, DMS-0352940
§ Department of Mathematics, North Carolina State University, Raleigh NC 27695
‖ Department of Mathematics, University of Nebraska, Lincoln, Lincoln NE 6858

The first computational algorithm was proposed in [19], in which the authors address the problem of locating a single line-segment crack from boundary data, as well as which types of input current fluxes yield the most stable estimates. In [18] the algorithm is demonstrated to be effective on experimentally collected data. The algorithm was extended to the multiple crack case in [13].

In [6] the "reciprocity gap" technique is used to develop a very simple algorithm for locating a single linear crack inside a conductor. The reciprocity gap approach has also found application in other inverse problems; see, for example [7], [9], and [10]. In [12] the authors adapt the reciprocity gap approach to construct an algorithm that can recover a collection of perfectly insulating linear cracks. The algorithm is easily adapted to the setting in which multiple input flux/boundary potential pairs are available. The authors also show how one may quantitatively deduce the number of cracks present from the boundary data.

In this paper we extend the algorithm of [12] to the case in which the cracks may be partially conductive. We also develop a variation on the algorithm that reduces the crack recovery problem to that of locating the simple poles and residues of a meromorphic function from boundary data. The connection between such meromorphic approximation problems and the impedance imaging problem for certain types of defects has been noted before, e.g., in [8] or [16]. In the latter paper the authors relate the problem of recovering a collection of small circular inclusions to the problem of identifying the poles and residues of a meromorphic function, and they propose a very simple algorithm to accomplish the latter task. We make use of that algorithm here. Our approach also relies on an asymptotic expansion of the potential with respect to the length of the cracks, in much the same spirit as the work in [4] and recent text [5].

The organization of the paper is as follows: in Section 2 we state the forward and corresponding inverse problem of interest, then review the reciprocity gap formulation. We also state our main theorem (Theorem 1) that, in conjunction with the reciprocity gap approach, allows us in Section 3 to develop our two algorithms for recovering a collection of cracks. We provide several computational examples, as well as concluding remarks. Section 4 is devoted to the proof of Theorem 1.

2. Mathematical Formulation of the Inverse Problem

2.1. The Forward Problem

Let Ω be a bounded region in $\mathbb{R}^2$ with C^2 boundary. We use Σ to denote a finite collection of closed, pair-wise disjoint line-segment "cracks" in Ω that do not intersect $\partial\Omega$, the boundary of Ω. Indeed, let us write $\Sigma = \cup_{j=1}^{n}\sigma_j$, where σ_j, the jth crack, is a line segment with center $p_j^* = (x_j^*, y_j^*) \in \Omega$. We use L_j to denote the length of σ_j, $\theta_j \in (-\pi/2, \pi/2]$ to denote the angle of σ_j with respect to horizontal, and $\mathbf{n}_j =< -\sin(\theta_j), \cos(\theta_j) >$ to denote a normal vector on the jth crack. Since our results depend on an asymptotic expansion in the limit that the crack lengths approach zero,

let us use Σ^ϵ to denote that collection of cracks in which σ_j has been contracted about p_j^* to length ϵL_j. When explicitly necessary, we will write σ_j^ϵ to denote the individual scaled cracks, and let $|\sigma_j^\epsilon| = \epsilon L_j$ denote the length of σ_j^ϵ. The parameter ϵ thus serves as a common scaling factor for the collection Σ. Note that changing ϵ doesn't change the crack centers p_j^* nor the crack orientations (hence normal vectors).

Let g denote an applied electrical flux on $\partial\Omega$ and $u^\epsilon \in H^1(\Omega \setminus \Sigma^\epsilon)$ the resulting electrical potential in Ω; for now we will explicitly indicate the dependence of the potential on ϵ with a superscript. We assume that u^ϵ is harmonic away from the cracks, and that $\frac{\partial u^\epsilon}{\partial \mathbf{n}} = g$ on $\partial\Omega$, where $\mathbf{n}$ is an outward-pointing unit normal vector field on $\partial\Omega$.

The boundary condition for u^ϵ on each crack is as follows: Let us denote the side into which $\mathbf{n}_j$ points as the "+" side of σ_j^ϵ and the other side as the "−" side. Since the cracks are assumed to present some resistance to the flow of current, the potential u^ϵ will not typically be continuous over any given crack. We use u_-^ϵ and u_+^ϵ to denote the limiting values for u^ϵ as we approach σ_j from the corresponding side, and set $[u^\epsilon] = u_+^\epsilon - u_-^\epsilon$ on each crack. Note that $[u^\epsilon]$ is well-defined in $H^{1/2}(\sigma_j^\epsilon)$ for each j, via an appropriate trace-operator. We assume that on each crack σ_j^ϵ the function u^ϵ satisfies $\frac{\partial u^\epsilon}{\partial \mathbf{n}_j} = k_j[u^\epsilon]$ for some constant $k_j \geq 0$, where the above equation must hold from both sides of σ_j^ϵ. For $k_j > 0$ this models the crack as a kind of "contact resistance" that allows the partial conduction of current in proportion to the potential difference across the crack. If $k_j = 0$ the crack blocks all current.

In summary, the potential u^ϵ satisfies

$$\begin{aligned}
\triangle u^\epsilon &= 0 \quad \text{in} \quad \Omega \setminus \Sigma^\epsilon && (1)\\
\frac{\partial u^\epsilon}{\partial \mathbf{n}} &= g \quad \text{on} \quad \partial\Omega && (2)\\
\frac{\partial u^\epsilon}{\partial \mathbf{n}_j} &= k_j[u^\epsilon] \quad \text{on} \quad \sigma_j && (3)\\
\int_{\partial\Omega} u^\epsilon \, ds &= 0. && (4)
\end{aligned}$$

The last condition enforces uniqueness of the solution, where ds indicates arc length on $\partial\Omega$.

It can be shown that there exists a unique solution $u^\epsilon \in H^1(\Omega \setminus \Sigma^\epsilon)$ to an appropriate weak formulation of equations (1)-(4); see, for example the appendix of [11]. The solution u^ϵ is of course smooth in $\Omega \setminus \Sigma^\epsilon$ and behaves as $\sqrt{r}$ near the crack tips, were r denotes distance to the crack tip. The gradient ∇u^ϵ behaves as $1/\sqrt{r}$.

Throughout the following analysis we use C to denote a constant that is independent of ϵ (but may depend on other crack parameters p_j^*, θ_j, k_j, as well as the domain Ω and applied flux g).

2.2. The Inverse Problem

The inverse problem is to recover the cracks and/or the transmission constants k_j given one or more input fluxes and the corresponding induced potentials on $\partial\Omega$. It was shown

in both [2] and [17] that two input flux/boundary-potential pairs of a certain form suffice to uniquely identify any collection of n perfectly insulating or conductive cracks (they need not be linear). The results can be extended to the present partial-conduction case.

In [6] the authors introduced the "reciprocity gap" principle, in which one attempts to locate a single insulating line-segment crack using (essentially) Green's second identity with the potential u and cleverly chosen test functions. A central portion of this computation is the recovery of the jump integral

$$\int_{\sigma^\epsilon} [u^\epsilon]\, ds$$

and related quantities over the crack. The technique is adapted in [12] to identify a finite collection of perfectly insulating cracks from one or more input fluxes. The approach also made use of an asymptotic approximation relating the crack centers and lengths to the jump integral over each crack. The harmonic test functions used are of the form $\phi(x, y) = e^{\eta(x+iy)}$ for a complex parameter η, similar to those that have been used to prove uniqueness in the more general impedance imaging problem, e.g., [14].

We adapt this technique to the present more general setting, and illustrate an alternate procedure for recovering the cracks that makes use of certain singular test functions related to the Green's function for the Laplacian.

2.3. Reciprocity Gap Formulation

Let v denote a harmonic function on Ω with suitably smooth boundary data. A simple application of the Divergence Theorem shows that

$$RG(v) := \int_{\partial\Omega} \left(u^\epsilon \frac{\partial v}{\partial \mathbf{n}} - v \frac{\partial u^\epsilon}{\partial \mathbf{n}} \right) ds = \sum_{j=1}^{n} \int_{\sigma_j^\epsilon} \frac{\partial v}{\partial \mathbf{n}_j} [u^\epsilon]\, ds. \tag{5}$$

The functional $RG(v)$ is the "reciprocity gap" functional; note $RG(v)$ can be computed from exterior boundary data. If no cracks are present we obtain $RG(v) = 0$ for all harmonic v. The details of the computation leading to equation (5) can be found in the appendix of [11], for the more general case in which $\frac{\partial u^\epsilon}{\partial \mathbf{n}} = F([u^\epsilon])$ on each crack, where F is some function which governs the transmission of current over the cracks.

In what follows we use u_0 to denote the harmonic function on Ω with Neumann data g (so u_0 is the potential with no cracks present, normalized to zero integral around $\partial\Omega$). Central to the reconstruction technique is the following Theorem.

Theorem 1 *Let u^ϵ denote the solution to the boundary value problem (1)-(4) for the collection Σ^ϵ, with centers p_j^*, normal vectors $\mathbf{n}_j$, transmission constants k_j, and crack lengths $|\sigma_j^\epsilon| = \epsilon L_j$. Assume that $|\nabla u_0(p_j^*)| > 0$ for each j. Then for any function v harmonic in Ω we have*

$$RG(v) = \sum_{j=1}^{n} \frac{\partial v}{\partial \mathbf{n}_j}(p_j^*) \frac{\partial u_0}{\partial \mathbf{n}_j}(p_j^*) \left(\frac{\frac{\pi}{4}|\sigma_j^\epsilon|^2}{1 + \frac{8k_j|\sigma_j^\epsilon|}{3\pi}} \right) + q(\epsilon) \tag{6}$$

where $|q(\epsilon)| \leq C\epsilon^4$ for some constant C that is independent of ϵ but may depend on Ω as well as the applied flux g, the crack centers and normal vectors, and transmission constants.

Remark 1 *For the purposes of reconstruction using Theorem 1 it is essential that the quantity $\frac{\partial u_0}{\partial \mathbf{n}_j}(p_j^*)$ be non-zero, and for this to occur we obviously require $\nabla u_0(p_j^*) \neq 0$. It is thus of interest to consider what types of input fluxes on the uncracked domain Ω yield harmonic functions u_0 with no interior critical points. Obvious possibilities are those input fluxes which yield linear solutions u_0. Alternatively, as can be deduced from the arguments in [2], any input flux of the form $g = \eta_0 - \eta_1$ in which $\eta_j \geq 0$, $\text{supp}(\eta_j) \subseteq \gamma_j \subset \partial\Omega$ with $\int_{\gamma_j} \eta_j \, ds = 0$, each γ_j connected, and $\gamma_0 \cap \gamma_1 = \emptyset$ yields a solution u_0 with no critical points. In a similar vein, as per the work in [17], one may also use a singular input flux of the form $g = \delta_P - \delta_Q$ (composed of Dirac delta functions) for distinct points P and Q in $\partial\Omega$.*

2.3.1. Example 1 We present a short example to illustrate the asymptotic expansion of Theorem 1. Let Ω be the unit disk and σ^ϵ a crack on the line $y = 0.1$, with endpoints $(0, 0.1)$ and $(0.2, 0.1)$, of length 0.2. Let the input flux be given by $g(\theta) = \sin(\theta)$, where $0 \leq \theta < 2\pi$ denotes angular position on $\partial\Omega$. We then have $u_0(x, y) = y$. Let the harmonic test function be given by $v(x, y) = y$. In this case (since $\frac{\partial u_0}{\partial y} = 1$ and $\frac{\partial v}{\partial y} = 1$ on σ^ϵ) we have, by equating the right side of equations (5) and (6), that

$$\int_{\sigma^\epsilon} [u^\epsilon] \, ds = \frac{\frac{\pi}{4}|\sigma^\epsilon|^2}{1 + \frac{8k|\sigma^\epsilon|}{3\pi}} + O(\epsilon^4).$$

Below we compare the left and right sides of the above equation (after dropping the $O(\epsilon^4)$ terms). For this example and those that follow we solve the boundary value problem (1)-(4) numerically by converting it into a system of integral equations supported on $\partial\Omega$ and Σ, which is then solved using Nyström's method (with a careful handling of the singularities near the crack tips). The solutions are accurate to about 4 significant figures, based on comparison to closed form solutions.

Table 2.3.1 shows the value of $\int_{\sigma^\epsilon}[u^\epsilon] \, ds$ as computed directly from our program versus the quantity $\frac{\frac{\pi}{4}|\sigma^\epsilon|^2}{1+\frac{8k|\sigma^\epsilon|}{3\pi}}$ for values of k from 0 to 50.

k	$\int_{\sigma^\epsilon}[u^\epsilon] \, ds$	$\frac{\frac{\pi}{4}\lvert\sigma^\epsilon\rvert^2}{1+\frac{8k\lvert\sigma^\epsilon\rvert}{3\pi}}$
0.0	0.0316	0.0314
1.0	0.0270	0.0269
3.0	0.0210	0.0208
5.0	0.0172	0.0170
10.0	0.0118	0.0116
20.0	0.0073	0.0071
50.0	0.0035	0.0033

Table 1: True vs. predicted jump integral, $|\sigma^\epsilon| = 0.2$.

The approximation (at least for this crack of length 0.2) appears to be good over a wide range for the transmission constant k.

In the next section we drop the negligible $O(\epsilon^4)$ terms in $RG(v)$, then demonstrate how one may easily recover the quantities p_j^* and $\mathbf{n}_j$ for each crack from $RG(v)$ by using suitably chosen test functions for v. We also recover the quantity $\left(\frac{\frac{\pi}{4}|\sigma_j^\epsilon|^2}{1+\frac{8k_j|\sigma_j^\epsilon|}{3\pi}}\right)$, from which we can recover the crack lengths $|\sigma_j^\epsilon|$.

3. Reconstruction Algorithm

3.1. Reconstruction from Complex Exponentials

3.1.1. A Single Input Flux In what follows we show how to recover the cracks in the case that the transmission constants k_j are known. We also make use of the correspondence $(x, y) \leftrightarrow x + iy$ between $\mathbb{R}^2$ and $\mathbb{C}$ when convenient. In [12] the authors used the reciprocity gap functional with test functions of the form $v_\eta(x, y) = -\frac{i}{\eta}e^{\eta(x+iy)}$ where $\eta \in \mathbb{C}, \eta \neq 0$. Note that v_η (complex-valued) is harmonic in the xy plane. If we insert v_η into equation (6), note that $|\sigma_j^\epsilon| = \epsilon L_j$, and drop the $O(\epsilon^4)$ terms we find that

$$\phi(\eta) := RG(v_\eta) = \sum_{j=1}^{n} A_j e^{p_j^*\eta} \tag{7}$$

with $p_j^* = x_j^* + iy_j^*$ the center of crack j and

$$A_j = \frac{\partial u_0}{\partial \mathbf{n}_j}(p_j^*)\left(\frac{\frac{\pi}{4}e^{i\theta_j}|\sigma_j^\epsilon|^2}{1+\frac{8k_j|\sigma_j^\epsilon|}{3\pi}}\right) \tag{8}$$

where recall θ_j denotes the angle of the jth crack. Above we also used the fact that the normal $\mathbf{n}_j$ on the jth crack is $\mathbf{n}_j =< -\sin(\theta_j), \cos(\theta_j) >$, so that $\nabla v_\eta(p_j^*) \cdot \mathbf{n}_j = e^{i\theta_j}e^{p_j^*\eta}$.

Given an input flux g and Dirichlet data u we have the ability to evaluate $\phi(\eta)$ for any non-zero choice of η. Moreover, one can easily see that the mth derivative $\phi^{(m)}(\eta)$ with respect to η may be computed "explicitly" from the boundary data as

$$\phi^{(m)}(\eta) = RG\left(\frac{\partial^m v_\eta(x, y)}{\partial \eta^m}\right)$$

(note $\frac{\partial^m v_\eta(x,y)}{\partial \eta^m}$ can be computed explicitly). However, it should be noted that although no explicit differencing of the boundary data is involved, for large m the function $\frac{\partial^m v_\eta}{\partial \eta^m}$ does become highly oscillatory in x and y. The computation of $\phi^{(m)}(\eta)$ may thus become ill-conditioned in the presence of noise if m is large.

With the ability to compute ϕ and its derivatives, we may attempt to recover the cracks as in [12]. Assume, just for the moment, that we know n, the number of

cracks present. The function $\phi(\eta)$ defined in equation (7) is a linear combination of n exponentials and so satisfies an nth order constant coefficient ODE

$$\phi^{(n)}(\eta) + c_{n-1}\phi^{(n-1)}(\eta) + \cdots c_1\phi'(\eta) + c_0\phi(\eta) = 0 \tag{9}$$

in which the p_j^* are the roots of the characteristic polynomial $r^n + c_{n-1}r^{n-1} + \cdots c_1 r + c_0 = 0$. We can thus recover the crack centers if we can determine the c_j. The c_j can be found by evaluating equation (9) for each of $\eta = \eta_m$, $1 \leq m \leq n$, (the η_m should of course be distinct) and then solving the resulting system of n linear equations in the n unknowns c_j, assuming the resulting system is of full rank. We could also use η_m for a larger set $1 \leq m \leq M$ with $M > n$; the over-determined system would be (in principle) consistent, but could be solved in a least-squares sense in any case.

With the c_j determined, the p_j^* are obtained as the roots of the characteristic polynomial for the ODE (9). We can obtain the coefficients A_j in equation (7) by evaluating $\phi(\eta_m)$ for $1 \leq m \leq n$ and solving the resulting linear system of n equations in n unknowns A_j. We can then use equation (8) to find

$$\theta_j = \arg(A_j) \tag{10}$$

with $-\pi/2 < \theta_j \leq \pi/2$ for each crack, and obtain the crack length by solving

$$|A_j| = \frac{\partial u_0}{\partial \mathbf{n}_j}(p_j^*)\left(\frac{\frac{\pi}{4}|\sigma_j^\epsilon|^2}{1 + \frac{8k_j|\sigma_j^\epsilon|}{3\pi}}\right) \tag{11}$$

for $|\sigma_j^\epsilon|$. Equation (11) is quadratic in $|\sigma_j^\epsilon|$ and has a unique positive root.

If the number of cracks is unknown but we have an upper bound N (so $n \leq N$) then we may posit the presence of N cracks and take $\phi(\eta)$ as a sum of the form (7), but with N terms rather than n (note, however, that only n of the terms will be non-zero). We then evaluate equation (9) for each of $\eta = \eta_m$, $1 \leq m \leq N$, which yields a system of N equations in N unknowns. However, if only n cracks are truly present, it's easy to see that the rank of the governing N by N matrix is exactly n. By computing the rank of this matrix we can deduce the actual number of cracks and proceed as before (while now solving the over-determined system obtained by inserting $\eta = \eta_m$, $1 \leq m \leq N$, into ϕ). Note, however, that this requires that each crack is "illuminated" by the input flux g, that is, that $\frac{\partial u_0}{\partial \mathbf{n}_j}(p_j^*) \neq 0$ for each j. Otherwise the crack is effectively invisible to our input flux, and $A_j \approx 0$.

Remark 2 *Of course it may be the case that $\frac{\partial u_0}{\partial \mathbf{n}_j}(p_j^*) = 0$ even though $\nabla u_0(p_j^*) \neq 0$, if the crack is locally parallel to ∇u_0. Since one does not know the crack orientation a priori, it can be beneficial to use two input fluxes, g_1 and g_2, which yield harmonic functions u_0^1 and u_0^2 with the property that $\nabla u_0^1(p)$ and $\nabla u_0^2(p)$ are not parallel at any point $p \in \Omega$. In much the same way as described in Remark 1, one can show that such flux pairs can be constructed. Specifically, one can deduce from the arguments in [2] that any input fluxes of the form $g_j = \eta_0 - \eta_j$ in which each $\eta_j \geq 0$, $\text{supp}(\eta_j) \subseteq \gamma_j \subset \partial\Omega$ with $\int_{\gamma_j} \eta_j \, ds = 0$, each γ_j connected, and the γ_j pairwise-disjoint, yield solutions u_0^1 and u_0^2 such that ∇u_0^1 and ∇u_0^2 are nowhere parallel (and from Remark 1, neither gradient*

vanishes at any point). And again, following the analysis in [17], one may also use singular input fluxes of the form $g_j = \delta_P - \delta_{Q_j}$, $j = 1, 2$ *for distinct points* Q_1, Q_2 *and* P *in* $\partial\Omega$.

Of course one can also use more than two fluxes. The effective use of data from multiple input fluxes is illustrated in Section 3.1.3.

3.1.2. Example 2 For this example we take, as in Example 1 above, Ω as the unit disk, a single input flux $g(\theta) = \sin(\theta)$, and all $k_j = 10$. We use three cracks with parameters as given in Table 2.

crack	p_j^*	angle	length
1	$(-0.4, 0.4)$	0.0	0.3
2	$(0.3, 0.6)$	-0.5	0.2
3	$(0.5, -0.6)$	0.7	0.2

Table 2: Crack Parameters, Example 2.

The boundary value problem (1)-(4) is solved numerically as previously described, with the solution u computed at 50 equally spaced points on $\partial\Omega$. All boundary integrals on $\partial\Omega$ are done with the trapezoidal rule (which is super-polynomially convergent on these types of integrands).

Let us use $N = 5$ as an upper bound on the number of cracks. We evaluate $\phi(\eta)$ and its derivatives at $\eta = e^{2\pi i j/5}$ for $j = 0$ to $j = 4$ and construct the matrix $\mathbf{M}$ obtained from equation (9). Figure 1 shows the magnitude of the singular values of $\mathbf{M}$:

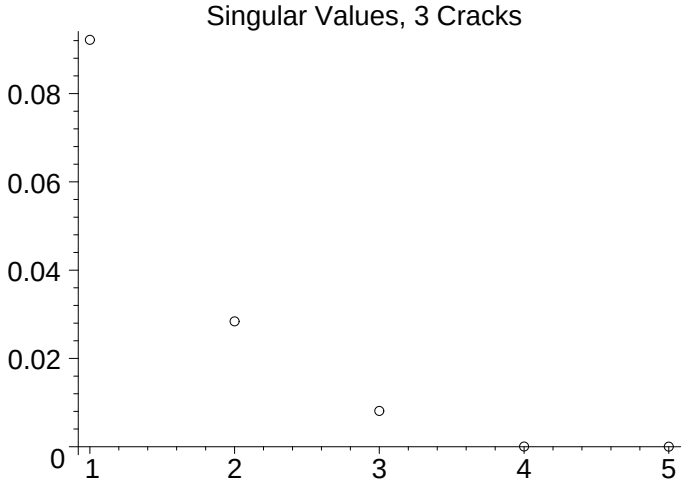

Figure 1: First 5 singular values of $\mathbf{M}$, 3 cracks.

In this (noise free) example, the first three singular values are within a factor of about 10 of each other, while the fourth singular value is 200 times smaller than the third.

We estimate the number of cracks by thresholding the singular values at a reasonable value, say five percent of the largest in magnitude (which we use for the remainder of this paper). In this case we correctly estimate that there are three cracks present.

We may now solve (in a least-squares sense) the system of five linear equations in three unknowns c_0, c_1, c_2 obtained by substituting $\eta = e^{2\pi ij/5}$ for $j = 0$ to $j = 4$ into equation (9). The result is $c_0 \approx 0.2514 - 0.1462i, c_1 \approx 0.1630 + .4325i, c_2 \approx -0.3678 - 0.3802i$. The roots of the cubic characteristic polynomial $r^3 + c_2 r^2 + c_1 r + c_0 = 0$ yield estimates

$$p_1^* \approx -0.42170 + 0.39593i, p_2^* \approx 0.2930 + 0.5789i, p_3^* \approx 0.4966 - 0.5946i,$$

reasonably close to the data from Table 2.

With the p_j^* in hand, we may substitute $\eta = e^{2\pi ij/5}$ for $j = 0$ to $j = 4$ into equation (7) and solve the resulting linear system (in a least-squares sense) for A_1, A_2, A_3. Doing so yields

$$A_1 \approx 0.01957 - 0.00217i, A_2 \approx 0.0100 - 0.0048i, A_3 \approx 0.0071 + 0.0059i.$$

By taking the arguments we estimate $\theta_1 \approx -0.011, \theta_2 \approx -0.448, \theta_3 \approx 0.695$. Finally, we may solve equation (11) with $k_j = 10$ (assumed known) for the crack lengths to obtain estimates

$$|\sigma_1| \approx 0.296, |\sigma_2| \approx 0.209, |\sigma_3| \approx 0.205.$$

Figure 2 shows both the original (heavier lines) and recovered (lighter) cracks.

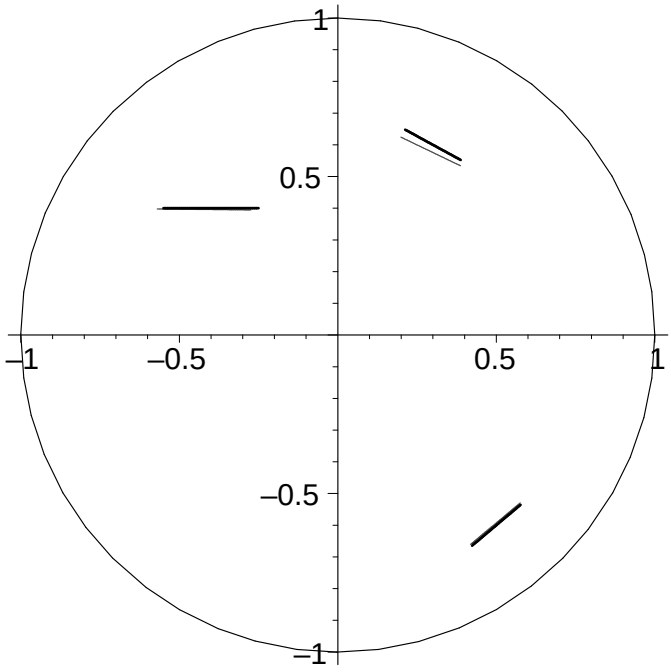

Figure 2: Original and recovered cracks.

The algorithm is particularly simple in the case of a single crack σ, for we can recover the center p^* as $p^* = \phi'(\eta)/\phi(\eta)$ for any $\eta \neq 0$ (within reason). We then take $A = \phi(\eta)e^{-p^*\eta}$, obtain the crack angle as $\theta = \arg(A)$ and the length by solving equation (11). The entire computation requires the evaluation of just two integrals over $\partial\Omega$ (and possibly the computation of $\frac{\partial u_0}{\partial \mathbf{n}}(p^*)$).

3.1.3. Multiple Input Fluxes The data obtained from multiple input fluxes is easily accommodated. Equation (7) makes it clear that the dependence of $\phi(\eta)$ on the input flux is through u_0 only, via the constants A_j. In particular, the terms $e^{p_j^*\eta}$ depend only on the crack centers. Let input fluxes g_r, $1 \leq r \leq R$ be applied, and let $\phi_r(\eta)$ denote the corresponding ϕ of equation (7). Each ϕ_r is a linear combination of precisely the same exponentials, $e^{p_j^*\eta}$, and hence satisfies exactly the same ODE (9).

We can thus proceed much as above to estimate the number of cracks and recover the c_j. Specifically, let $N \geq n$ be an upper bound on the number of cracks and let $\mathbf{M}_r$ denote the N by N matrix governing the system obtained by evaluating (9) at N distinct points $\eta = \eta_m$, $1 \leq m \leq N$. The "stacked" system we obtain by amalgamating the $\mathbf{M}_r$ as

$$\mathbf{M} = [\mathbf{M}_1^T \ \ \mathbf{M}_2^T \ \ \cdots \ \ \mathbf{M}_R^T]^T \tag{12}$$

(with a similar stacking operation performed on the right hand side of the linear systems) has the c_j as the solution. Moreover, the rank of $\mathbf{M}$ is still n, the actual number of cracks present. We may thus estimate n as above, solve for the c_j, and recover the crack centers p_j^*.

The quantity A_j varies with the input flux, but we may estimate it for any particular input flux g_r and then employ (10) and (11). We may also use different fluxes to estimate the angle and length of each crack. However, the stability of the resulting estimates for any given crack may vary widely depending on which input flux is used. We will address this issue below, for a different class of test functions, and also provide an example of a reconstruction using multiple input fluxes.

3.2. Reconstruction from Singular Test Functions

Let $\eta = \alpha + i\beta \in \partial\Omega$ and define the complex-valued harmonic function

$$v_\eta(x, y) = \frac{1}{2\pi} \ln(z - \eta)$$

(with $z = x + iy$) for $z \neq \eta$, with the branch cut for the log taken on a curve tangent to the outward unit normal to $\partial\Omega$ at η and otherwise not intersecting Ω (so that v_η will be harmonic in Ω). In (r, θ) polar coordinates centered at η, the real part of v_η is given by $\frac{1}{2\pi}\ln(r)$ (the usual Green's function for the Laplacian) while the imaginary part of v_η is given by the argument θ, branch cut as above. The use of such a singular test function in the reciprocity gap approach has been considered before, for the case of a single crack, in [3].

The function v_η is not regular enough to put in $RG(v_\eta)$ directly, but a rather standard potential theory argument (exclude a small ϵ-ball around η, apply Green's second identity, limit ϵ to zero) shows that

$$-\frac{1}{2}u^\epsilon(\eta) + \text{p.v.} \int_{\partial\Omega} \left(u^\epsilon \frac{\partial v_\eta}{\partial \mathbf{n}} - v_\eta g \right) ds = \sum_{j=1}^{n} \int_{\sigma_j^\epsilon} \frac{\partial v_\eta}{\partial \mathbf{n}_j} [u^\epsilon] \, ds \tag{13}$$

where the integral over $\partial\Omega$ must be interpreted in the sense of principal value due to a $1/(z-\eta)$ singularity in $\frac{\partial v_\eta}{\partial \mathbf{n}}$.

Let $\psi(\eta)$ denote the left side of equation (13). In light of Theorem 1 and a bit of straightforward algebra we can approximate the right side of (13) (after dropping $O(\epsilon^4)$ terms; note v_η is smooth inside Ω) to obtain

$$\psi(\eta) = \sum_{j=1}^{n} \frac{B_j}{z - p_j^*} \tag{14}$$

where

$$B_j = -\frac{1}{8} \frac{\partial u_0}{\partial \mathbf{n}_j}(p_j^*) \left(\frac{i e^{i\theta_j} |\sigma_j^\epsilon|^2}{1 + \frac{8k_j |\sigma_j^\epsilon|}{3\pi}} \right). \tag{15}$$

Recall, we have the ability to compute $\psi(\eta)$ for any $\eta \in \partial\Omega$. This reduces the crack identification problem to one of recovering the (simple) poles and residues of a meromorphic function in a domain from boundary information.

A very simple and efficient algorithm for solving this problem (along with some stability analysis) is given in [16]. To briefly review, the authors show that for a function ψ as defined by equation (14), if one defines

$$c_m = \frac{1}{2\pi i} \int_{\partial\Omega} z^m \psi(z) \, dz$$

(note c_m is computable from the boundary data) then $c_m = \sum_{j=1}^{n} B_j (p_j^*)^m$. Moreover, the c_m satisfy a recurrence relation

$$c_{m+j} + R_1 c_{m+j-1} + \cdots + R_n c_j = 0$$

for $j \geq 0$, where the p_j^* are the roots of the nth degree polynomial

$$z^n + R_1 z^{n-1} + \cdots R_{n-1} z + R_n = 0. \tag{16}$$

They thus propose an algorithm for recovering the c_m, as follows (suppose for the moment we know n): First, solve the linear equation

$$\begin{bmatrix} c_0 & c_1 & \cdots & c_{n-1} \\ c_1 & c_2 & \cdots & c_n \\ \vdots & \vdots & & \vdots \\ c_{n-1} & c_n & \cdots & c_{2n-2} \end{bmatrix} \begin{bmatrix} R_n \\ R_{n-1} \\ \vdots \\ R_1 \end{bmatrix} = \begin{bmatrix} -c_n \\ -c_{n+1} \\ \vdots \\ -c_{2n-1} \end{bmatrix} \tag{17}$$

for the coefficients R_j. The p_j^* are then the solutions to equation (16). The residues B_j can be found from

$$\begin{bmatrix} 1 & 1 & \cdots & 1 \\ p_1^* & p_2^* & \cdots & p_n^* \\ \vdots & \vdots & & \vdots \\ (p_1^*)^{n-1} & (p_2^*)^{n-1} & \cdots & (p_n^*)^{n-1} \end{bmatrix} \begin{bmatrix} B_1 \\ B_2 \\ \vdots \\ B_n \end{bmatrix} = \begin{bmatrix} c_0 \\ c_1 \\ \vdots \\ c_{n-1} \end{bmatrix}. \tag{18}$$

We can then obtain the crack angle from equation (15), as $\theta_j = \arg(B_j) + \pi/2$. The crack length can be obtained by taking the magnitude of both sides of equation (15) and solving for $|\sigma_j^\epsilon|$.

If the number of cracks/poles is not known, we form the matrix on the left in equation (17) using an upper bound N on the number of cracks in place of n. The authors in [16] outline a procedure for estimating the true number of cracks/poles. This procedure involves the determinants of the upper left m by m submatrices of the matrix in equation (17) and certain tolerances concerning the minimum distance between the poles and the size of the residues. For simplicity, we will simply use the thresholded singular values of the matrix, as we did above, to estimate the rank of the matrix (which is the number of cracks present).

3.2.1. Numerical Example We use the same domain Ω and same three cracks as in Example 2 (refer to Table 2). We'll use input flux $g(\theta) = \sin(\theta)$ again and transmission constants $k_j = 10$. The boundary value problem (1)-(4) is solved numerically as previously described, with the solution u computed at 50 equally spaced points on $\partial\Omega$.

We take upper bound $N = 5$ on the number of cracks and form the corresponding matrix on the left in equation (17). The singular values turn out to be $6.6152 \times 10^{-3}, 2.3376 \times 10^{-3}, 1.2482 \times 10^{-3}, 1.919 \times 10^{-5}, 7.039 \times 10^{-6}$. Thresholding at 5 percent of the largest singular value yields the (correct) estimate of three cracks; the drop from the third to fourth singular value is almost two orders of magnitude. A plot of the singular values is similar to Figure 1.

The solution to equation (17) with $n = 3$ is $R_1 \approx 0.2560 - 0.1504i, R_2 \approx 0.1643 + 0.4212i, R_3 \approx -0.3710 - 0.3812i$. The roots from equation (16) are then

$$p_1^* \approx -0.427 + .390i, \quad p_2^* \approx 0.307 + 0.588i, \quad p_3^* \approx 0.492 - 0.597i.$$

All are reasonably close. The residues from equation (18) are $B_1 \approx -1.524 \times 10^{-4} - 3.057 \times 10^{-3}i, B_2 \approx -6.762 \times 10^{-4} - 1.493 \times 10^{-3}i, B_3 \approx 9.694 \times 10^{-4} - 1.108 \times 10^{-3}i$. As per the remarks after equation (18), we recover angles

$$\theta_1 \approx -0.05, \quad \theta_2 \approx -0.43, \quad \theta_3 \approx 0.72$$

and estimated lengths

$$|\sigma_1| \approx 0.292, \quad |\sigma_2| \approx 0.196, \quad |\sigma_3| \approx 0.208.$$

Figure 3 shows the true (heavier, darker) and recovered (lighter) cracks.

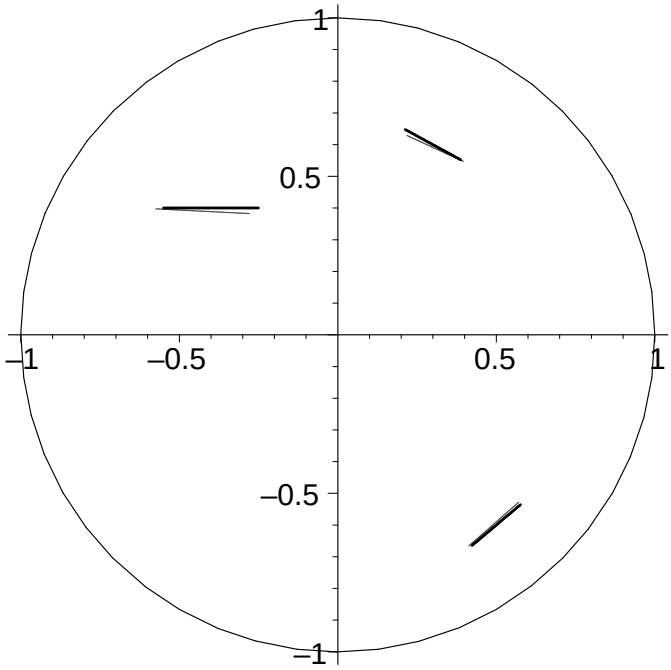

Figure 3: Original and recovered cracks.

3.2.2. Multiple Input Flux Example The singular test function approach is also easily adapted to handle multiple input fluxes. Each input flux/Dirichlet data pair from the forward problem gives rise to a meromorphic function of the form (14). Let N be an upper bound on the number of cracks present. If we have R input fluxes let these meromorphic functions be denoted $\psi_1, \ldots, \psi_R$. Note that all ψ_j have exactly the same poles, merely differing residues at each pole. Let $\mathbf{M}_j$ denote the matrix on the left side of (17) corresponding to ψ_j, $\mathbf{b}_j$ the right side of (17), and as before let $\mathbf{M}$ be the matrix constructed as in equation (12), and $\mathbf{b} = [\mathbf{b}_1^T \cdots \mathbf{b}_R^T]^T$. It's easy to see that $\mathbf{R} = [R_1, \ldots, R_N]^T$ satisfies $\mathbf{MR} = \mathbf{b}$ and as before, that the rank of $\mathbf{M}$ is the true number of cracks n. We can then restrict to the case $N = n$ and solve $\mathbf{MR} = \mathbf{b}$ (in a least-squares sense). We then recover the crack centers from equation (16) as before.

Each input flux gives rise to a different set of residues, however, differing only in the $\frac{\partial u_0}{\partial \mathbf{n}}$ factor in front. A flux that yields a larger value for the residue B_j corresponding to the jth crack should yield more stable estimates for the angle and length of that crack (an issue examined more closely in [12]). This is not surprising, since the ideal situation is that in which ∇u_0 is locally parallel to $\mathbf{n}$ on the crack; the worst case is ∇u_0 orthogonal to $\mathbf{n}$, so the current flux sweeps over the crack undisturbed. As such, we may use each input flux individually to estimate the residues corresponding to the jth crack, select the largest magnitude residue, and use that to estimate the length and angle of the jth crack.

We now implement this strategy for the domain and cracks of the previous example, but with the third crack at an angle of 1.3 radians with respect to horizontal and the additional input flux $g_2(\theta) = \cos(\theta)$. We also add Gaussian random noise to each of the 50 data points, with mean zero and standard deviation 0.0001, about 2 percent of the maximum value of $|u - u_0|$ for either flux on $\partial\Omega$ (a realistic noise level for impedance data). With an upper bound $N = 5$ on the number of cracks we find that the singular values of the relevant ten by five matrix $\mathbf{M}$ are as shown in Figure 4:

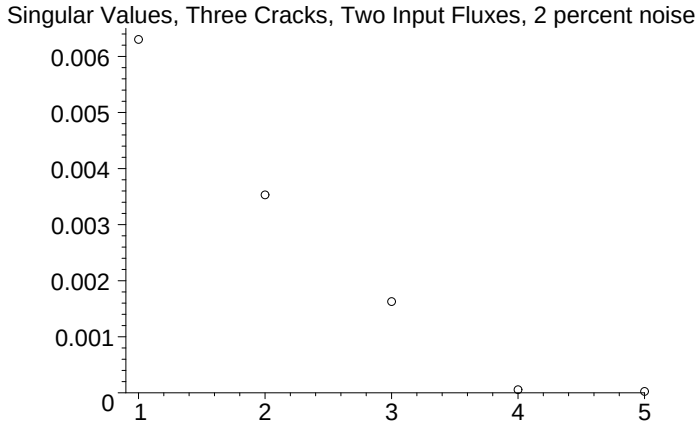

Figure 4: Singular values, three cracks, two input fluxes.

Thresholding at five percent of the largest singular value again yields an estimate of three cracks.

The (least-squares) solution to the system $\mathbf{MR} = \mathbf{b}$ described above is $R_1 \approx 0.2551 - 0.1572i, R_2 \approx 0.1688 + 0.4126i, R_3 \approx -0.3807 - 0.3530i$. The crack centers obtained by solving equation (16) are

$$p_1^* \approx -0.434 + 0.383i, \quad p_2^* \approx 0.323 + 0.578i, \quad p_3^* \approx 0.492 - 0.608i.$$

We now use each flux individually (with the p_j^* as above) to estimate the residue at $z = p_j^*$ for that flux using equation (18). We find that the first input flux $g(t) = \sin(\theta)$ yields residues of magnitudes $3.02 \times 10^{-3}, 1.64 \times 10^{-3}$, and 5.15×10^{-4} at p_1^*, p_2^*, and p_3^*, respectively. The estimated residue magnitudes for the second flux $\cos(\theta)$ are $9.32 \times 10^{-5}, 8.85 \times 10^{-4}$, and 1.79×10^{-3}, respectively. We thus use the residues for the first input flux to estimate the length and angle of the cracks centered at p_1^* and p_2^*, and the residue for the second flux to estimate these quantities for the crack centered at p_3^*. Proceeding as above, we find

$$\theta_1 \approx -0.08, \quad \theta_2 \approx -0.37, \quad \theta_3 \approx 1.33$$

and estimated lengths

$$|\sigma_1| \approx 0.290, \quad |\sigma_2| \approx 0.193, \quad |\sigma_3| \approx 0.223.$$

Figure 4 shows the original and recovered cracks.

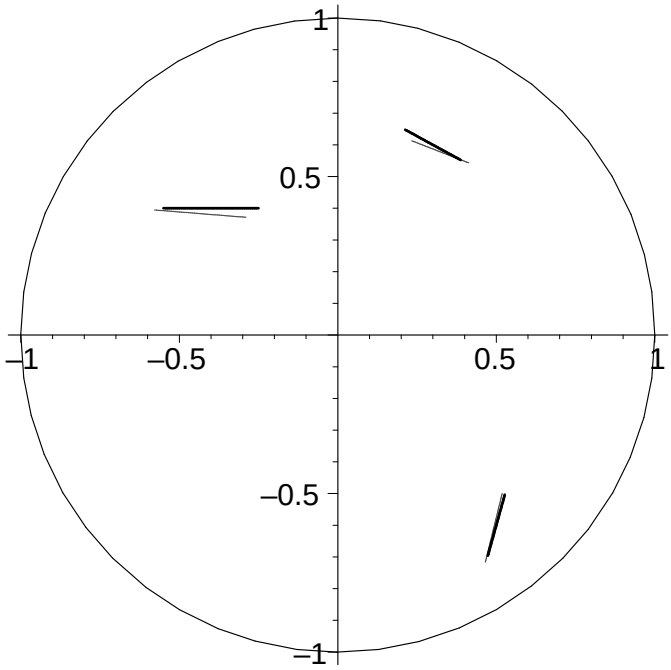

Figure 4: Original and recovered cracks, two input fluxes, 2 percent noise.

3.3. Conclusions

The two approaches, using complex-exponential and Green's functions, are obviously quite similar; both reduce the problem of locating the crack centers to that of finding the roots of the same polynomial. They might be considered equivalent via the "Laplace Transform" relation $e^{pt} \leftrightarrow \frac{1}{z-p}$.

Our approach for determining the crack lengths requires a priori knowledge or estimates of the transmission constants on each crack, for of course the relation (8) allows one to solve only for $|\sigma_j^\epsilon|$ or k_j. Note, however, that locating the crack centers and angles does not depend on this knowledge. A more refined expansion than that given in Theorem 1 is undoubtedly possible—the information that would allow simultaneous determination of both quantities lives in the $O(\epsilon^4)$ terms (and would involve the second derivatives of u_0). Simultaneous determination of both would likely be quite unstable.

It would be quite interesting to adapt some version of Theorem 1 and the reciprocity gap approach to the full heat equation. It also seems likely that some adaptation of this approach should work on 3D problems with "penny-shaped" planar cracks (or other similar geometric constraints), at least with the complex-exponential test functions. The singular test function approach, however, ultimately relies on the interpretation of the problem in terms of meromorphic functions, and may not have a convenient generalization.

4. Proof of Theorem 1

4.1. Preliminary Lemma

For the moment we shall focus on the case in which a single crack σ is present. Without loss of generality we choose coordinates so that σ has center $p^* = (0,0)$ and normal $\mathbf{n} = (0,1)$. Let ϵ denote the length of σ, so σ spans the range $-\epsilon/2 \leq x \leq \epsilon/2$ on the x axis. For simplicity we will not explicitly notate the dependence of the crack and corresponding solution u to equations (1)-(4) on ϵ. The transmission constant will be denoted by k.

Since σ is presumed to be short, we expect that $u = u_0 + v$ for some "small" function v (recall u_0 is harmonic in Ω, the solution to (1)-(4) when no crack is present). The function $v \in H^1(\Omega \setminus \sigma)$ must be harmonic on $\Omega \setminus \sigma$ with zero Neumann data on $\partial\Omega$ and satisfy

$$\frac{\partial v}{\partial y}(x,0) - k[v](x) = -\frac{\partial u_0}{\partial y}(x,0) \tag{19}$$

for $-\epsilon/2 < x < \epsilon/2$ (where $\frac{\partial v}{\partial y}(x,0)$ takes the same limiting value from both sides of σ).

Let us cast the problem for v in a weak form, but with the assumption that $\frac{\partial v}{\partial \mathbf{n}} = h$ is not necessarily zero on $\partial\Omega$. An integration by parts yields

$$\int_{\Omega\setminus\sigma} \nabla\phi \cdot \nabla v \, dx = -\int_\sigma [\phi] \left(k[v] - \frac{\partial u_0}{\partial y} \right) ds + \int_{\partial\Omega} \phi h \, ds \tag{20}$$

for all suitably smooth (e.g. $H^1(\Omega \setminus \sigma)$) functions ϕ on $\Omega \setminus \sigma$.

We will begin by constructing a solution v to the weak form (20) in which h is "small," as quantified by the following Lemma. In what follows we assume the applied flux g is such that $|\nabla u_0(p^*)| > 0$.

Lemma 1 *There exists a function $v \in H^1(\Omega \setminus \sigma)$ that satisfies equation (20) with Neumann data h on $\partial\Omega$ with supremum norm $\|h\|_\infty$ bounded as*

$$\|h\|_\infty \leq C\epsilon^2$$

for some constant C (C may depend on the applied flux g through u_0, as well as the crack center and orientation, and transmission constant k, but not ϵ). Moreover, $[v]$ on σ has an expansion

$$\begin{aligned}[v](x) = &\frac{\epsilon}{1 + \frac{8k\epsilon}{3\pi}} \frac{\partial u_0}{\partial y}(p^*) \sqrt{1 - 4x^2/\epsilon^2} + \frac{\partial^2 u_0}{\partial y \partial x}(p^*) \frac{\epsilon^2}{8} U_1(2x/\epsilon) \sqrt{1 - 4x^2/\epsilon^2} \\ &+ \frac{\partial u_0}{\partial y}(p^*) \sum_{m=2}^{\infty} \frac{8k(-1)^{m+1}\epsilon^2}{\pi(m+1)^2(m+3)(m-1)} U_m(2x/\epsilon) \sqrt{1 - 4x^2/\epsilon^2} \\ &+ R(\epsilon, x)\end{aligned} \tag{21}$$

where $|R(\epsilon,x)| \leq C\epsilon^3$ for some C (independent of x and ϵ) and $U_m(x)$ denotes the m degree Chebyshev polynomial of the second kind on $[-1,1]$.

It's worth noting that the terms involving $U_m(2x/\epsilon)\sqrt{1-4x^2/\epsilon^2}$ for $m \geq 1$ in the expansion (21) are indeed of order $O(\epsilon^2)$ in the supremum norm, for $|U_m(2x/\epsilon)\sqrt{1-4x^2/\epsilon^2}| \leq 1$ for $-\epsilon/2 \leq x \leq \epsilon/2$, which follows from the substitution $2x/\epsilon = \cos(t)$ and identity $U_m(\cos(t)) = \sin((m+1)t)/\sin(t)$ (see [1], chapter 22).

Proof of Lemma 1: When convenient we will make the identification $z = x+iy = (x,y)$ between $\mathbb{C}$ and $\mathbb{R}^2$. Define the function $\phi(z) = -z+(z+1)\sqrt{\frac{z-1}{z+1}}$ for $z \in \mathbb{C}\setminus[-1,1]$, with the square-root branch cut on the negative real axis; note ϕ is analytic on $\mathbb{C}\setminus[-1,1]$ and maps this domain to the interior of the unit ball in $\mathbb{C}$. Straightforward series expansions show that for any $C > 1$ we have

$$|\phi(z)| \leq \frac{C}{|z|}, \quad |\phi'(z)| \leq \frac{C}{4|z|^2} \tag{22}$$

for all sufficiently large $|z|$.

Let $\phi_j(x,y) = \mathrm{Im}(\phi^{j+1}(x+iy))$ for $j \geq 0$. The ϕ_j are harmonic on $z \in \mathbb{C}\setminus[-1,1]$ and as shown in [11] (Lemma 4.1, with change of variable $z \to 2z-1$) we have

$$[\phi_j](x) = 2(-1)^j U_j(x)\sqrt{1-x^2}, \tag{23}$$

$$\frac{\partial \phi_j}{\partial y}(x) = (j+1)(-1)^{j+1}U_j(x), \tag{24}$$

for $-1 \leq x \leq 1$, where $[\phi_j](x) = \lim_{y\to 0^+}(\phi_j(x,y) - \phi_j(x,-y))$ and U_j denotes the jth degree Chebyshev polynomial of the second kind on $[-1,1]$. The $U_j(x)$ are orthogonal on $[-1,1]$ with respect to the weight function $\sqrt{1-x^2}$, with $\int_{-1}^{1} U_j^2(x)\sqrt{1-x^2}\,dx = \pi/2$ for $j \geq 0$. It is easy to deduce from (22) that for any $C > 1$ we have

$$|\phi_j(x,y)| \leq \left(\frac{C}{4}\right)^{j+1} \frac{1}{|x+iy|^{j+1}}, \quad |\nabla\phi_j(x,y)| \leq \left(\frac{C}{4}\right)^{j+1} \frac{j+1}{|x+iy|^{j+2}} \tag{25}$$

for all sufficiently large $|x+iy|$.

Given that ϕ maps $\mathbb{C}\setminus[-1,1]$ to the interior of the unit ball in $\mathbb{C}$, we see that $|\phi_j| \leq 1$ in $\mathbb{C}\setminus[-1,1]$; it is straightforward to check that $\lim_{(x,y)\to(-1,0)}\phi_j(x,y) = 1$, $\lim_{(x,y)\to(1,0)}\phi_j(x,y) = -1$, and that $\phi_j \in H^1(D\setminus[-1,1])$ for any bounded region $D \subset \mathbb{R}^2$ which contains $[-1,1]$ (for ϕ_j, like ϕ, has a $\sqrt{r}$ singularity near $z=-1$ and $z=1$, while $\nabla\phi_j$ has a $1/\sqrt{r}$ singularity).

Indeed, we can bound the norm of ϕ_j in $H^1(D\setminus[-1,1])$. A straightforward application of the divergence theorem shows that

$$\int_{B_R(0)\setminus[-1,1]} |\nabla\phi_j|^2\,dx = \int_{|z|=R} \phi_j \frac{\partial\phi_j}{\partial\mathbf{n}}\,ds - \int_{-1}^{1}[\phi_j]\frac{\partial\phi_j}{\partial\mathbf{n}}\,dx.$$

The last integral, from conditions (23) and (24), is just $-(j+1)\pi$, while the first integral on the right above tends to zero as $R \to \infty$. We conclude that $\|\nabla\phi_j\|_{L^2(D\setminus[-1,1])} \leq \sqrt{(j+1)\pi}$ on any bounded domain D, and so clearly we may bound

$$\|\phi_j\|_{H^1(D\setminus[-1,1])} \leq C\sqrt{(j+1)\pi} \tag{26}$$

for some constant C.

We will construct a solution to equation (19) as a superposition of the ϕ_j. Let us first rewrite equation (19) by noting that

$$\begin{aligned}-\frac{\partial u_0}{\partial y}(x,0) = & -\frac{\partial u_0}{\partial y}(0,0) - \frac{\partial^2 u_0}{\partial y \partial x}(0,0)x - \frac{\partial^3 u_0}{\partial y \partial x^2}(x^*,0)x^2 \\ & = \frac{\partial u_0}{\partial y}(0,0)(-1+\alpha x + r(x))\end{aligned}$$

for some x^* between 0 and x, where $x \in (-\epsilon/2, \epsilon/2)$, $\alpha = -\frac{\partial^2 u_0}{\partial y \partial x}(0,0)/\frac{\partial u_0}{\partial y}(0,0)$ and $r(x) = -\frac{\partial^3 u_0}{\partial y \partial x^2}(x^*,0)x^2/\frac{\partial u_0}{\partial y}(0,0)$. We also have bounds

$$|r(x)| \le Cx^2, \quad |r'(x)| \le Cx \tag{27}$$

The constant C depends on the crack center $p^* = (0,0)$, domain Ω, and flux g (through u_0).

The solution v to equation (19) can be written $v(x,y) = \frac{\partial u_0}{\partial y}(0,0)w(x,y)$ where w is harmonic on $\Omega \setminus \sigma$ and satisfies

$$\frac{\partial w}{\partial y}(x,0) - k[w](x) = -1 + \alpha x + r(x) \tag{28}$$

for $x \in (-\epsilon/2, \epsilon/2)$. We will take w in the form

$$w(x,y) = \sum_{j=0}^{\infty} c_j \phi_j(2x/\epsilon, 2y/\epsilon) \tag{29}$$

for appropriate constants c_j.

To determine the c_j (formally for the moment, analytical justification to follow), we insert w as defined in (29) above into equation (28) and make use of equations (23) and (24) to obtain

$$\sum_{j=0}^{\infty} c_j p_j(x) = -1 + \alpha x + r(x). \tag{30}$$

for $-\epsilon/2 < x < \epsilon/2$, where

$$p_j(x) = (-1)^{j+1} U_j(2x/\epsilon)\left(\frac{2(j+1)}{\epsilon} + 2k\sqrt{1-4x^2/\epsilon^2}\right). \tag{31}$$

Multiply both sides of equation (30) by $U_m(2x/\epsilon)\sqrt{1-4x^2/\epsilon^2}$ for fixed $m \ge 0$ and integrate on $-\epsilon/2 \le x \le \epsilon/2$ (note $\int_{-\epsilon/2}^{\epsilon/2} U_j^2(2x/\epsilon)\sqrt{1-4x^2/\epsilon^2}\,dx = \frac{\pi}{4}\epsilon$ for all j). A formal interchange of the sum and integrals followed by division by $\frac{\pi}{2}(-1)^{m+1}(m+1)$ yields

$$c_m + k\sum_{j=0}^{\infty} B_{mj} c_j = a_m + b_m \tag{32}$$

for $0 \le m < \infty$, where

$$B_{mj} = \frac{4(-1)^{j-m}}{(m+1)\pi} \int_{-\epsilon/2}^{\epsilon/2} U_j(2x/\epsilon) U_m(2x/\epsilon)(1-4x^2/\epsilon^2)\,dx \tag{33}$$

$$a_0 = \frac{\epsilon}{2}, \quad a_1 = \frac{\alpha\epsilon^2}{16}, \quad a_m = 0 \ \text{ for } \ m \ge 2, \tag{34}$$

$$b_m \quad = \frac{2(-1)^{m+1}}{\pi(m+1)} \int_{-\epsilon/2}^{\epsilon/2} U_m(2x/\epsilon) r(x) \sqrt{1-4x^2/\epsilon^2}\, dx \tag{35}$$

and we have used $\int_{-\epsilon/2}^{\epsilon/2} U_m(2x/\epsilon)\sqrt{1-4x^2/\epsilon^2}\, dx = \frac{\pi}{4}\epsilon$ for $m = 0$, zero otherwise, and $\int_{-\epsilon/2}^{\epsilon/2} xU_m(2x/\epsilon)\sqrt{1-4x^2/\epsilon^2}\, dx = \frac{\pi}{16}\epsilon^2$ for $m = 1$, zero otherwise.

The B_{mj} can in fact be worked out explicitly; the substitution $2x/\epsilon = \cos(t)$ with the standard identity $U_j(\cos(t)) = \sin((j+1)t)/\sin(t)$ converts the integral to a workable form and we find that $B_{mj} = 0$ if $j+m$ is odd, while

$$B_{mj} = \frac{8\epsilon(j+1)}{\pi(j+m+1)(j+m+3)(j-m+1)(m-j+1)} \tag{36}$$

if $j+m$ is even. Note that $B_{mj} \le 0$ for $m \ne j$, while $B_{mm} = \frac{8\epsilon(m+1)}{\pi(2m+1)(2m+3)} > 0$.

It will be convenient to bound $|b_m|$ in terms of m. If we make the same substitution as above, $2x/\epsilon = \cos(t)$, in the integral of (35) we obtain

$$b_m = \frac{\epsilon(-1)^{m+1}}{\pi(m+1)} \int_0^{\pi} \sin((m+1)t)\sin(t) r(\epsilon\cos(t)/2)\, dt.$$

Two applications of integration by parts to take a derivative off of $\sin((m+1)t)$ (or $\cos((m+1)t)$) terms and put the derivative onto the rest of the integrand (all endpoint terms vanish) easily yields

$$|b_m| \le \frac{C\epsilon^3}{(m+1)^3} \tag{37}$$

for some constant C independent of m and ϵ, if we use the bounds (27).

Claim 1: *For all $\epsilon > 0$ and all $k \ge 0$ the system (32) is uniquely solvable in l^∞, the space of bounded sequences of real numbers (which we index from 0).*

To see this write the system (32) in the form

$$(\mathbf{D} + \tilde{\mathbf{B}})\mathbf{c} = \mathbf{a} + \mathbf{b} \tag{38}$$

where $\mathbf{D}$ is the diagonal operator with entries $D_{mm} = 1 + kB_{mm}$, $\tilde{\mathbf{B}}$ is the operator with entries $\tilde{B}_{mj} = kB_{mj}$ for $m \ne j$, diagonal $\tilde{B}_{mm} = 0$), $\mathbf{c} = (c_0, c_1, \ldots) \in l^\infty$, and similarly for $\mathbf{a}$, $\mathbf{b}$.

It's easy to see that $\mathbf{D}$ is well-defined on l^∞, with operator norm $\|\mathbf{D}\| = 1 + kB_{00} = 1 + \frac{8k\epsilon}{3\pi}$. The operator $\tilde{\mathbf{B}}$ is also well-defined on l^∞, for a rather unenlightening induction argument shows that

$$\sum_{j=0}^{\infty} |\tilde{B}_{mj}| = \frac{2k\epsilon(4m^3+8m^2+4m+1)}{\pi(2m+1)(2m+3)(m+1)^2}, \quad m \text{ even} \tag{39}$$

$$\sum_{j=0}^{\infty} |\tilde{B}_{mj}| = \frac{2k\epsilon(4m^3+8m^2-3)}{\pi m(m+2)(2m+1)(2m+3)}, \quad m \text{ odd} \tag{40}$$

By taking the largest numerator (that of (39)) and the smaller denominator (that of (40)) we see that

$$\sum_{j=0}^{\infty} |\tilde{B}_{mj}| \leq q(m) := \frac{2k\epsilon(4m^3+8m^2+4m+1)}{\pi m(m+2)(2m+1)(2m+3)}. \tag{41}$$

One may verify that $q'(m) < 0$ for all $m > 0$ (treating m as a real variable). We then have $q(m) \leq q(2) = \frac{73k\epsilon}{140\pi}$ for $m \geq 2$, while equation (39) for $m = 0$ yields $\frac{2k\epsilon}{3\pi}$ and equation (40) for $m = 1$ yields $\frac{2k\epsilon}{5\pi}$. Thus all row sums for $\tilde{\mathbf{B}}$ are bounded by $\frac{2k\epsilon}{3\pi}$, so that $\|\tilde{\mathbf{B}}\| \leq \frac{2k\epsilon}{3\pi}$ and $\tilde{\mathbf{B}}$ is a bounded operator on l^∞.

To show that $\mathbf{D} + \tilde{\mathbf{B}}$ is invertible with bounded inverse, let $\mathbf{R} = \mathbf{D}^{-1}\tilde{\mathbf{B}}$. We will show that the operator norm $\|\mathbf{R}\|$ satisfies $\|\mathbf{R}\| < 1$, so that $(\mathbf{I} + \mathbf{R})$ has a bounded inverse (via a Neumann series, $(\mathbf{I} + \mathbf{R})^{-1} = \mathbf{I} - \mathbf{R} + \mathbf{R}^2 - \cdots$). It will then follow that $(\mathbf{D} + \tilde{\mathbf{B}})^{-1} = \mathbf{D}^{-1}(\mathbf{I} + \mathbf{R})^{-1}$. Note that $\|\mathbf{D}^{-1}\| \leq 1$.

To see that $\|\mathbf{R}\| < 1$, note that the row sums of $\mathbf{R}$ can be bounded by making use of equation (41) as

$$\begin{aligned} \sum_{j=0}^{\infty} |R_{mj}| &= \frac{1}{D_{mm}} \sum_{j=0}^{\infty} |\tilde{B}_{mj}| \\ &\leq \frac{q(m)}{1 + \frac{8\epsilon k(m+1)}{\pi(2m+1)(2m+3)}} \end{aligned} \tag{42}$$

at least for $m \geq 1$. We can write the right side of (42) as

$$h(t) = \frac{at}{1 + \frac{a}{L}t}$$

where $t = k\epsilon$, $a = \frac{2(4m^3+8m^2+4m+1)}{\pi m(m+2)(2m+1)(2m+3)}$, and $L = \frac{4m^3+8m^2+4m+1}{4m^3+12m^2+8m} < 1$ for all $m \geq 1$. The function $h(t)$ is positive with $\lim_{t\to\infty} h(t) = L$; moreover, for any fixed t and a the function h is strictly increasing with respect to L, so that $h(t) < \frac{at}{1+at} < 1$. We conclude that $h(k\epsilon) < 1$, that is, $\sum_{j=0}^{\infty} |R_{mj}| < 1$, for $m \geq 1$. In the special case $m = 0$ we have $\sum_{j=0}^{\infty} |R_{0j}| = \frac{2k\epsilon}{3\pi+8k\epsilon} < 1/4$. It follows that $\|\mathbf{R}\| < 1$ for all positive k, ϵ, which proves Claim 1.

Note that we can also obtain a bound more useful for $\epsilon \approx 0$ and any fixed k, specifically,

$$\|\mathbf{R}\| \leq \|\mathbf{D}^{-1}\|\|\tilde{\mathbf{B}}\| \leq \frac{2k\epsilon}{3\pi} \tag{43}$$

using the bound $\|\tilde{\mathbf{B}}\| \leq \frac{2k\epsilon}{3\pi}$ from above. Also, given that $(\mathbf{D} + \tilde{\mathbf{B}})^{-1}$ is bounded and in view of the definition (34) and the bound (37) we find

$$\|\mathbf{c}\|_\infty = \|(\mathbf{D} + \tilde{\mathbf{B}})^{-1}(\mathbf{a} + \mathbf{b})\| \leq C\|\mathbf{a} + \mathbf{b}\|_\infty \leq C\epsilon \tag{44}$$

for some constant C.

Claim 2: *We have* $|c_0| \leq C\epsilon$, $|c_1| \leq C\epsilon^2$, *and*

$$|c_m| \leq \frac{C\epsilon^2}{(m+1)^3} \tag{45}$$

for $m \geq 2$ *and some constant* C *(which may depend on* k*).*

The bound $|c_0| \leq C\epsilon$ is immediate from (44). For the bounds on $|c_m|$ for $m \geq 1$ first note that from equation (32)

$$(1 + kB_{mm})c_m = a_m + b_m - k \sum_{j=0, j\neq m}^{\infty} B_{mj}c_j$$

From the triangle inequality

$$(1 + kB_{mm})|c_m| \leq |a_m| + |b_m| + k \left| \sum_{j=0}^{\infty} B_{mj}c_j \right| \tag{46}$$

$$\leq |b_m| + k \left| \sum_{j=0, j\neq m}^{\infty} B_{mj}c_j \right| \quad \text{if} \quad m \geq 2. \tag{47}$$

The last inequality follows since $a_m = 0$ for $m \geq 2$. Note that from equation (34) we have $a_0 = \epsilon/2$ and $a_1 = O(\epsilon^2)$ so in light of the bound (37), we need only show that the sum on the right in (47) is bounded by $\frac{C\epsilon^2}{(m+1)^3}$ (this will suffice to show the bound on $|c_1|$ as well).

It's easy to see from the bound (41) that the mth row sum of $\tilde{\mathbf{B}}$ can be bounded by $Ck\epsilon/(m+1)$ for some C (since the numerator is cubic in m, the denominator quartic) so that

$$k \left| \sum_{j=0, j\neq m}^{\infty} B_{mj}c_j \right| \leq \frac{Ck^2\epsilon}{m+1} \|\mathbf{c}\|_\infty \leq \frac{Ck^2\epsilon^2}{m+1}$$

(by virtue of (44)) for some C, so that from (46) and (47) we have for all $m \geq 1$ that

$$|c_m| \leq \frac{Ck^2\epsilon^2}{(m+1)(1 + \frac{8k\epsilon}{3\pi})} \leq \frac{Ck^2\epsilon^2}{(m+1)}. \tag{48}$$

Now let us examine the sum $\sum_{j=0}^{\infty} B_{mj}c_j$ again in light of the bound (48). We have (using $B_{mm} > 0$, $B_{mj} \leq 0$ for $j \neq m$)

$$\left| \sum_{j=0}^{\infty} B_{mj}c_j \right| \leq \left(B_{mm}|c_m| - |B_{m0}||c_0| - \sum_{j=1, j\neq m}^{\infty} B_{mj}|c_j| \right) \tag{49}$$

From (36) it's easy to bound

$$|B_{mj}| \leq \frac{C\epsilon(j+1)}{(m+1)^2(m-j)^2} \quad \text{and} \quad B_{mm} \leq \frac{C\epsilon}{m+1}$$

for $j \neq m$, $j, m \geq 0$, which in conjunction with (47), (48), (49) and $\sum_{j=1}^{\infty} 1/j^2 < \infty$ yields

$$|c_m| \leq \frac{Ck^2\epsilon^2}{(m+1)^2} \tag{50}$$

for $m \geq 1$. Finally, the same "bootstrap" argument with (50) in place of (48) proves Claim 2 (with the constant $C = Ck^2$).

Claim 3: *The function w defined by equation (29) satisfies*

$$\int_{\Omega\setminus\sigma} \nabla\phi \cdot \nabla w \, dx = -\int_{\sigma} [\phi] \left(k[w] + (-1 + \alpha x + r(x))\right) \, ds \tag{51}$$

for any $\phi \in H^1(\Omega \setminus \sigma)$ with ϕ supported away from $\partial\Omega$. That is to say, w satisfies the weak form of $\triangle w = 0$ in $\Omega \setminus \sigma$ with the boundary condition (28) on σ.

To prove this let $L^2_w(\sigma)$ denote the space of square-integrable function on the crack $\sigma = [-\epsilon/2, \epsilon/2]$ with respect to weight function $\sqrt{1 - 4x^2/\epsilon^2}$. The c_j as determined in fact provide a solution to equation (30) in $L^2_w(\sigma)$. To see this, first note that the $p_j(x)$ as defined by equation (31) are in $L^2_w(\sigma)$, and one can easily check that $\|p_j\|_{L^2_w} \leq C(j+1)$ for some constant C. Given the rate of decay of the c_j from equation (45) the function

$$p(x) = \sum_{j=0}^{\infty} c_j p_j(x) \tag{52}$$

is well-defined $L^2_w(\sigma)$. Moreover, we find from equation (30) that $< p(x), U_m(2x/\epsilon >_w = < -1 + \alpha x + r(x), U_m(2x/\epsilon >_w$, where $<, >_w$ denotes the $L^2_w(\sigma)$ inner product and term-by-term integration is permissible since p is square-integrable. Thus the c_j as computed do indeed yield a solution to equation (30) in $L^2_w(\sigma)$.

In fact, the sum in (52) is well-defined in the un-weighted space $L^2(\sigma)$. To see this, note

$$\int_{-\epsilon/2}^{\epsilon/2} p_j^2(x) \, dx \leq C\epsilon(j+1)\ln(j+1) \tag{53}$$

follows easily from the definition (31) and the estimate

$$\int_{-1}^{1} U_j^2(x) \, dx = 2\int_0^{\pi/2} \frac{\sin^2((j+1)t)}{\sin(t)} \, dt \leq C\int_0^{\pi/2} \frac{\sin^2((j+1)t)}{t} \, dt = \gamma + \ln(j\pi) - \mathrm{Ci}(j\pi).$$

where we use the substitution $x = \cos(t)$ again, exploit the symmetry of the integral about $t = \pi/2$, and the fact that $\sin(t) \geq \frac{2}{\pi}t$ on this interval. Here γ is Euler's constant and the definition of Ci may be found in [1], chapter 5. Since $\mathrm{Ci}(t)$ approaches zero as $t \to \infty$ we obtain the bound (53). Given the bound (45), we find that since $\sum_{j=1}^{\infty} \ln(j)/j^2 < \infty$, the sum on the right in (52) converges in $L^2(\sigma)$. Thus p provides a solution to equation (30) in $L^2(\sigma)$.

Define w according to equation (29), and let

$$w_n(x,y) = \sum_{j=0}^{n} c_j \phi_j(2x/\epsilon, 2y/\epsilon).$$

Given the bound (26) (which also holds for $\phi_j(2x/\epsilon, 2y/\epsilon)$) and the rate of decay (45) of the c_j with respect to j we find that $w_n \to w \in H^1(\Omega \setminus \sigma)$. Boundedness of the trace operator $\phi \to [\phi]$ from $H^1(\Omega \setminus \sigma)$ to $L^2(\sigma)$ shows that $[w_n] \to [w]$ in $L^2(\sigma)$.

Note that

$$\frac{\partial w_n}{\partial y}(x,0) - k[w_n] = \sum_{j=0}^{n} p_j(x)$$

for $x \in (-\epsilon/2, \epsilon/2)$. An integration by parts for any $\phi \in H^1(\Omega \setminus \sigma)$ with ϕ supported away from $\partial\Omega$ yields

$$\int_{\Omega\setminus\sigma} \nabla\phi \cdot \nabla w_n \, dx = -\int_{\sigma} [\phi] \left(k[w_n] + \sum_{j=0}^{n} c_j p_j(x) \right) ds.$$

We may pass to the limit in n above and make use of the fact that $\sum_{j=0}^{n} c_j p_j$ converges to $-1 + \alpha x + r(x)$ (the right side of (30)), while $[w_n] \to [w]$ in $L^2(\sigma)$ to obtain (51), which proves Claim 3.

We can now finish the proof of Lemma 1. It's easy to see from the bounds (25) that $\frac{\partial w}{\partial \mathbf{n}}$ is well-defined (pointwise) on $\partial\Omega$, and satisfies $|\frac{\partial w}{\partial \mathbf{n}}| \leq C\epsilon^2$ at each point on $\partial\Omega$.

To establish the asymptotic expansion (21), note that the solution $\mathbf{c}$ to equation (38) can be split as $\mathbf{c} = \mathbf{c}^a + \mathbf{c}^b$ where $(\mathbf{D} + \tilde{\mathbf{B}})\mathbf{c}^a = \mathbf{a}$ and $(\mathbf{D} + \tilde{\mathbf{B}})\mathbf{c}^b = \mathbf{b}$. From (37) and the boundedness of $(\mathbf{D} + \tilde{\mathbf{B}})^{-1}$ we obtain $\|\mathbf{c}^b\|_\infty \leq C\epsilon^3$ for some constant C. Thus the dominant $O(\epsilon)$ and $O(\epsilon^2)$ portions of the solution come from $\mathbf{c}^a$.

From $(\mathbf{D} + \tilde{\mathbf{B}})\mathbf{c}^a = \mathbf{D}(\mathbf{I} + \mathbf{R})\mathbf{c}^a = \mathbf{a}$ we have $(\mathbf{I} + \mathbf{R})\mathbf{c}^a = \mathbf{D}^{-1}\mathbf{a}$. Application of the Neumann series for $(\mathbf{I} + \mathbf{R})^{-1}$ yields

$$\mathbf{c}^a = \mathbf{D}^{-1}\mathbf{a} - \mathbf{R}\mathbf{D}^{-1}\mathbf{a} + \sum_{j=2}^{\infty} (-1)^j \mathbf{R}^j \mathbf{D}^{-1}\mathbf{a}.$$

From the bound (43) the latter sum is dominated by $C\epsilon^3$ in the supremum norm. Indeed, given the definition of $\mathbf{D}$ and $\mathbf{R}$ we find that to order ϵ^2 we have

$$\begin{aligned} c_0^a &= \frac{\epsilon/2}{1 + \frac{8k\epsilon}{3\pi}} \\ c_1^a &= \frac{\alpha\epsilon^2}{16} \\ c_m^a &= -\frac{4k\epsilon^2}{\pi(m+1)^2(m+3)(m-1)}, \quad m \geq 2 \end{aligned}$$

The same expansion in ϵ holds for c_1, c_2, and c_m. In light of equations (23), (29), and the decay rate of the c_m with respect to m we find that

$$\begin{aligned}[w](x) = &\frac{\epsilon}{1+\frac{8k\epsilon}{3\pi}}\sqrt{1-4x^2/\epsilon^2} - \frac{\alpha\epsilon^2}{8}U_1(2x/\epsilon)\sqrt{1-4x^2/\epsilon^2} \\ &+ \sum_{m=2}^{\infty}\frac{8k(-1)^{m+1}\epsilon^2}{\pi(m+1)^2(m+3)(m-1)}U_m(2x/\epsilon)\sqrt{1-4x^2/\epsilon^2} \\ &+ R(\epsilon,k,x) \end{aligned} \tag{54}$$

for $-\epsilon/2 \le x \le \epsilon/2$, where $|R(\epsilon,x)| \le C\epsilon^3$ for some C (independent of x and k for k in any neighborhood of 0). (Note that all terms of the form $U_m(2x/\epsilon)\sqrt{1-4x^2/\epsilon^2}$ are bounded between -1 and 1.).

Finally, from $v(x,y) = \frac{\partial u_0}{\partial y}(p^*)w(x,y)$, (29), and (54) (and recall $\alpha = -\frac{\partial^2 u_0}{\partial y \partial x}(p^*)/\frac{\partial u_0}{\partial y}(p^*)$) we obtain equation (21). This completes the proof of Lemma 1.

4.2. Proof of Theorem 1

To complete the proof of Theorem 1, we now suppose Ω has n cracks as described in section 2.1. The remainder of the proof is quite similar to that of Lemma 1 in section 5.2 of [12]. Indeed, the following Lemma can be demonstrated in exactly the same manner as Lemma 4 in [12]. We omit the proof.

Lemma 2 *Let Ω be a bounded region in $\mathbb{R}^2$ and $\Sigma^\epsilon = \cup_{j=1}^n \sigma_j^\epsilon$, with each σ_j^ϵ a line segment with center $p_j^* \in \Omega$, at angle θ_j and with length ϵL_j. Let $\phi^\epsilon \in H^1(\Omega \setminus \Sigma^\epsilon)$ satisfy $\triangle\phi^\epsilon = 0$ in $\Omega \setminus \Sigma^\epsilon$ with $\frac{\partial\phi^\epsilon}{\partial \mathbf{n}} = h_0$ on $\partial\Omega$, $\frac{\partial\phi^\epsilon}{\partial \mathbf{n}} - k_j[\phi^\epsilon] = h_j$ on σ_j^ϵ with $\frac{\partial\phi^\epsilon}{\partial \mathbf{n}}$ continuous across σ_j^ϵ, with $h_0 \in L^2(\partial\Omega)$ and $h_j \in L^2(\sigma_j)$. Assume ϕ^ϵ has been normalized so that $\int_{\partial\Omega}\phi^\epsilon\, ds = 0$. Then*

$$\|\phi^\epsilon\|_{H^1(\Omega\setminus\Sigma^\epsilon)} \le C\left(\|h_0\|_{L^2(\partial\Omega)} + \sum_{j=1}^n \|h_j\|_{L^2(\sigma_j^\epsilon)}\right)$$

where C is independent of $\epsilon > 0$ for all sufficiently small ϵ.

For each integer j with $1 \le j \le n$ let v_j denote the function v in Lemma 1 appropriate to the crack σ_j (rotated and translated, of course). Set

$$V(x,y) = \sum_{j=1}^n v_j(x,y).$$

Note that each v_j is smooth away from σ_j, and in particular v_j is smooth over σ_k for $k \ne j$. From Lemma 1 and the bound (25) we can clearly obtain bounds

$$|\nabla v_j(x,y)| \le \frac{C\epsilon^2}{|(x,y)-\sigma_j|^2} \quad \text{and} \quad |\nabla V(x,y)| \le \frac{C\epsilon^2}{|(x,y)-\sigma_j|^2} \tag{55}$$

where $|(x,y)-\sigma_j|$ denotes the distance from the point (x,y) to crack σ_j and C is independent of ϵ and (x,y), provided we restrict (x,y) to any fixed subset of Ω which excludes a neighborhood of each crack center. The function V is harmonic on $\mathbb{R}^2 \setminus \Sigma$.

Now define the function $u_1(x,y) = u_0(x,y) + V(x,y)$ on $\Omega \setminus \Sigma$ (recall u_0 is the solution to (1)-(4) with no cracks present). The function u_1 is harmonic on $\Omega \setminus \Sigma$ and in light of (55) and the construction of the v_j we have

$$\frac{\partial u_1}{\partial \mathbf{n}} = g + h_0 \text{ on } \partial\Omega$$
$$\frac{\partial u_1}{\partial \mathbf{n}} = k_j[u_1] + h_j \text{ on } \sigma_j, \quad 1 \le j \le n$$

where $h_j = \sum_{m \neq j} \frac{\partial v_m}{\partial \mathbf{n}}|_{\sigma_j}$, so that $\|h_j\|_\infty \le C\epsilon^2$ for some C, $0 \le j \le n$. The function u_1 is "almost" the solution to (1)-(4), except for the h_j discrepancies.

Let w_0 denote the harmonic function on Ω with Neumann data $\frac{\partial w_0}{\partial \mathbf{n}} = -h_0$ on $\partial\Omega$. Note that standard elliptic estimates show that $|\nabla w_0(x,y)| \le C\epsilon^2$ for $(x,y) \in \Omega$. Let w_j, $1 \le j \le n$, denote the analogue of the v_j constructed above but with w_0 replacing u_0. It's easy to see from the expansion (21) of Lemma 1 and $|\nabla w_0(x,y)| \le C\epsilon^2$ that

$$|[w_j]| \le C\epsilon^3 \tag{56}$$

on σ_j, while $|\frac{\partial w_j}{\partial \mathbf{n}}| \le C\epsilon^4$ on σ_m for $m \neq j$. Define $W(x,y) = \sum_j w_j(x,y)$ and set $u_2 = u_0 + V + w_0 + W$. The function u_2 is harmonic on $\Omega \setminus \Sigma$ and satisfies $\frac{\partial u_2}{\partial \mathbf{n}} - k_j[u_2] = 0$ on each σ_j, while $\frac{\partial u_2}{\partial \mathbf{n}} = h$ on $\partial\Omega$ with $\|h\|_\infty \le C\epsilon^4$ on $\partial\Omega$. Finally, let $\phi \in H^1(\Omega \setminus \Sigma)$ be the solution to (1)-(4) but with Neumann data $\frac{\partial \phi}{\partial \mathbf{n}} = -h$ on $\partial\Omega$. Lemma 2 shows that $\|\phi\|_{H^1(\Omega\setminus\Sigma)} \le C\epsilon^4$ for some C. It follows from standard trace inequalities that

$$\|[\phi]\|_{L^2(\sigma_j)} \le C\epsilon^4 \tag{57}$$

The function $u_2 + \phi$ is exactly the solution to (1)-(4) with the Neumann data g, so that $u = u_2 + \phi = u_0 + V + w_0 + W + \phi$. Moreover, on any crack σ_j we have

$$[u] = [V] + [W] + [\phi] = [v_j] + [w_j] + [\phi]$$

since u_0 and w_0 are harmonic (hence have zero jumps). From the bound (56) we have $\|[w_j]\|_{L^\infty(\sigma_j)} \le C\epsilon^3$. We may use equation (21), along with the bounds (57) and (56) to conclude that if σ_j is parameterized in arc length s for $s = -\epsilon L_j/2$ to $s = \epsilon L_j/2$ (so the center p_j^* is at $s = 0$) we have

$$\begin{aligned}
[u](s) = {} & \frac{\epsilon}{1 + \frac{8k_j\epsilon}{3\pi}} \frac{\partial u_0}{\partial \mathbf{n}}(p^*)\sqrt{1 - 4L_j^2 s^2/\epsilon^2} \\
& + \frac{\partial^2 u_0}{\partial \tau \partial \mathbf{n}}(p^*)\frac{\epsilon^2}{8} U_1(2L_j s/\epsilon)\sqrt{1 - 4L_j^2 s^2/\epsilon^2} \\
& + \frac{\partial u_0}{\partial \mathbf{n}}(p^*) \sum_{m=2}^{\infty} \frac{8k(-1)^{m+1}\epsilon^2}{\pi(m+1)^2(m+3)(m-1)} U_m(2L_j s/\epsilon)\sqrt{1 - 4L_j^2 s^2/\epsilon^2} \\
& + R_1(\epsilon, s) + R_2(\epsilon, s)
\end{aligned} \tag{58}$$

where τ is a unit tangent vector to σ_j, $|R_1(\epsilon,s)| \le C\epsilon^3$ and $\|R_2(\epsilon,\cdot)\|_{L^2(-\epsilon/2,\epsilon/2)} \le C\epsilon^4$.

Let $\phi(x,y)$ be any smooth "test" function and consider the integral

$$J := \int_{\sigma_j} [u] \frac{\partial \phi}{\partial \mathbf{n}}\, ds = \int_{-\epsilon/2}^{\epsilon/2} [u](s) \frac{\partial \phi}{\partial \mathbf{n}}(s)\, ds \tag{59}$$

We may expand

$$\frac{\partial \phi}{\partial \mathbf{n}}(s) = \frac{\partial \phi}{\partial \mathbf{n}}(p_j^*) + \frac{\partial^2 \phi}{\partial \mathbf{n} \partial \tau}(p_j^*)s + E_j(s) \tag{60}$$

where $|E_j(s)| \leq Cs^2$ for some constant C independent of the cracks provided the cracks lie in some compact subset of Ω (certainly the case if ϵ is sufficiently small). If we use equation (60) to replace $\frac{\partial \phi}{\partial \mathbf{n}}(s)$ in the right side of (59) and equation (58) to replace $[u](s)$ we find

$$J = \frac{\partial \phi}{\partial \mathbf{n}}(p_j^*) \frac{\partial u_0}{\partial \mathbf{n}}(p_j^*) \left(\frac{\frac{\pi}{4}\epsilon^2 L_j^2}{1 + \frac{8k_j \epsilon L_j}{3\pi}} \right) + q(\epsilon) \tag{61}$$

where $|q(\epsilon)| \leq C\epsilon^4$. This last fact follows if one uses that the functions $U_m(2s/\epsilon)$ are orthogonal with respect to the weight function $\sqrt{1 - 4s^2/\epsilon^2}$, $U_1(s) = s$, and the bounds on the functions $R_1(\epsilon, s), R_2(\epsilon, s)$, and $E_j(s)$.

The proof of Theorem 1 follows immediately by superposition and equation (61).

5. References

[1] Abramowitz, Milton and Irene Stegun, *Handbook of mathematical functions*, Applied Mathematics Series, vol. 55. Washington: National Bureau of Standards, 1964. Reprinted 1968 by Dover Publications, New York.

[2] Alessandrini, F., and Diaz Valenzuela, A., *Unique determination of multiple cracks by two measurements*, Siam J Cont Opt, 34 (3), 1996, pp. 913-921.

[3] Alves, C., Abdallah, J., and Jaoua, M., *Recovery of cracks using a point-source reciprocity gap function*, 4th International Conference on Inverse Problems in Engineering, Rio de Janeiro, Brazil, 2002.

[4] Ammari, H., Moskow, S., and Vogelius, M., Boundary integral formulae for the reconstruction of electric and electromagnetic inhomogeneities of small volume. ESAIM: Cont. Opt. Calc. Var., 9 (2003), pp. 49–66.

[5] Ammari, H., and Kang, H., *Reconstruction of Small Inhomogeneities from Boundary Measurements*, Springer-Verlag, Lecture Notes in Mathematics, Volume 1846, 2004.

[6] Andrieux, S., and Ben Abda, A., *Identification de fissures planes par une donneé de bord unique; un procédé direct de localisation et d'identification*, , C.R. Acad. Sci., Paris I, 1992, **315**, pp 1323-1328.

[7] Bannour, T., Ben Abda, A., and Jaoua, M., *A semi-explicit algorithm for the reconstruction of 3D planar cracks*, Inverse Problems, **13** (4), 1997, pp. 899-917.

[8] Baratchart, L., Leblond, J., Mandréa, F., and Saff, E.B., *How can the meromorphic approximation help to solve some 2D inverse problems for the Laplacian?*, Inverse Problems, **15**, 1999, pp. 79-90.

[9] Ben Abda, A., Ben Ameur, H., and Jaoua, M., *Identification of 2D cracks by elastic boundary measurments*, Inverse Probl, **15** (1), 1999, pp. 67-77.

[10] Ben Abda, A., Chaabane, S., Dabaghi, F. El, and Jaoua, M., *On a non-linear geometrical inverse problem of Signorini type: Identifiablity and stability*, Math Method Appl Sci, **21** (15), 1998, pp. 1379-1398.

[11] Bryan, K., Ogborne, R., and Vellela, M., *Reconstruction of cracks with unknown transmission condition from boundary data*, Inverse Problems, 21, 2005, pp. 239-256.

[12] Bryan, K., Krieger, R., and Trainor, N., *Imaging of multiple linear cracks using impedance data*, to appear in the Journal of Computational and Applied Mathematics. Preprint available at `www.rose-hulman.edu/~bryan/reu2/mulcracks.pdf`.

[13] Bryan, K., Liepa, V., and Vogelius, M., Reconstruction of multiple cracks from experimental electrostatic boundary measurements, Inverse Problems and Optimal Design in Industry, 7, 1993, pp. 147-167.

[14] Calderón, A.P., *On an inverse boundary value problem*, Seminar on Numerical Analysis and Its Applications to Continuum Physics, (Rio de Janeiro, 1980), pp. 65-73, Soc. Brasil Mat., Rio de Janeiro, 1980.

[15] Friedman, A., and Vogelius, M., *Determining cracks by boundary measurements*, Ind U Math J, **38**, 1989, pp. 527-556.

[16] Kang, H., and Lee, H., *Identification of simple poles via boundary measurements and an application of EIT*, Inverse Problems, 20, 2004, pp. 1853-1863.

[17] Kim, H., and Seo, J., *Unique determination of a collection of a finite number of cracks from two boundary measurements*, Siam J. Math. Anal. **27**, 1996, pp. 1336-1340.

[18] Liepa, V., Santosa, F., and Vogelius, M., *Crack determination from boundary measurements—reconstruction using experimental data*, J. Nondestructive Evaluation, **12**, 1993, pp.163-174.

[19] Santosa, F., and Vogelius, M., *A computational algorithm to determine cracks from electrostatic boundary measurements*, Int J Engr Sci, **29**, 1991, pp. 917-937.